



# Renormalized chemical kinetics and benchmark quantum mechanical rates: activation energies and tunnelling transivities for the reactions of fluorine atoms with H<sub>2</sub> and HD

Valter H. Carvalho-Silva<sup>1,2</sup> · Flávio O. Sanches-Neto<sup>2,3,4</sup> · Guilherme M. Leão<sup>1</sup> · Simonetta Cavalli<sup>5</sup> · Dario De Fazio<sup>6</sup> · Maria C. Nucci<sup>7,8</sup> · Vincenzo Aquilanti<sup>5,6</sup>

Received: 15 September 2023 / Accepted: 24 October 2023 / Published online: 6 December 2023  
© The Author(s) 2023

## Abstract

Experimental, theoretical and computational chemical kinetics contribute to progress both in molecular and materials sciences and in biochemistry, exploring the gap between elementary processes and complex systems. Stationary state quantum mechanics and statistical thermodynamics provide interpretive tools and instruments for classical molecular dynamics simulations for stable or metastable structures and near-equilibrium situations. Chemical reaction kinetics plays a key role at the mesoscales: time-dependent and evolution problems are typically tackled phenomenologically, and reactions through intermediates and transition states need be investigated and modelled. In this paper, scaling and renormalization procedures are developed beyond the Arrhenius equation and the Transition State Theory, regarding two key observables in reaction kinetics, the rate “constant” as a function of temperature (and its reciprocal, the generalised lifetime), and the apparent activation energy (and its reciprocal, the transitivity function). Coupled first-order equations—dependent on time and on temperature—are formulated in alternative coupling scheme they link experimental results to effective modelling, or vice versa molecular dynamics simulations to predictions. The passage from thermal to tunnelling regimes is uniformly treated and applied to converged quantum mechanical calculations of rate constants available for the prototypical three-atom reactions of fluorine atoms with both H<sub>2</sub> and HD: these are exothermic processes dominated by moderate tunnel, needing formal extension to cover the low-temperature regime where aspects of universal behaviour are shown to emerge. The results that have been validated towards experimental information in the 10–350 K temperature range, document the complexity of commonly considered “elementary” chemical reactions: they are relevant for modelling atmospheric and astrophysical environments. Perspectives are indicated of advances towards other types of transitions and to a global generality of processes of interest in applied chemical kinetics in biophysics and in astrochemistry.

**Keywords** Quantum mechanical converged rate constants · Scaled and renormalized time and temperature variables · Arrhenius and *sub*-Arrhenius regimes · Transition state theory and TST · Aquilanti–Mundim formula

## Chemical symbols

|           |   |
|-----------|---|
| a, b, c   | Stoichiometric coefficients   |
| A, B      | Compositions of reacting species  |
| C         | Composition of a product species  |
| R         | Composition of representative reactant  |
| $\hat{R}$ | Compositions of species R as a general function of time $t$ and temperature $T$ |

|           |   |
|-----------|---|
| $d$       | Deformation parameter, see Eq. (17a, 17b)               |
| $E_a$     | Apparent activation energy, a function of $T$ .         |
| $k_B$     | Boltzmann constant                                      |
| $\hat{k}$ | Reaction rate constant, of time $t$ and temperature $T$ |
| $k$       | Reaction rate constant, a function of temperature $T$   |

## Greek letters

|                                   |   |
|-----------------------------------|---|
| $\alpha = 1/\varepsilon^\ddagger$ | Reciprocal of ideal activation energy, see (Carvalho-Silva et al. 2019) |
| $\beta = 1/k_B T$                 | Lagrange coldness parameter   |

This peer-reviewed research paper belongs to the Topical Collection originated from contributions to the conference held in Rome, March 27–28, 2023, promoted by Accademia Nazionale dei Lincei and Fondazione Guido Donegani on Chemical Kinetics at Micro-, Meso-, Bioscales, dedicated to Gianguualberto Volpi (1928–2017, Linceo from 1994).

Extended author information available on the last page of the article

|   |   |
|---|---|
| $\beta^\ddagger$                          | Marginal Lagrange coldness parameter for heating/freezing                               |
| $\hat{\gamma}$                            | Transitivity, a function of time $t$ and temperature $T$                                |
| $\gamma = 1/E_a$                          | Transitivity, a function of temperature $T$   |
| $\delta = \tan^{-1}(-d)$                  | From inversion of Eq. (7b)  |
| $\varepsilon = k_B T$                     | Kinetic energy  |
| $\varepsilon^\ddagger = 1/\beta^\ddagger$ | Marginal energy for heating/freezing  |
| $\varepsilon^\ddagger$                    | Arrhenius–Eyring energy barrier   |
| $\zeta$                                   | Universality class exponent at transition between Arrhenius and low-temperature regimes |
| $\nu$                                     | Pseudomolecularity exponent, see Eq. (17a, 17b)   |
| $\rho$                                    | Generalised reaction order, stoichiometric coefficient of R                             |
| $\hat{\tau} = 1/\hat{k}$                  | Generalised lifetime, Eq. (15), a function of time $t$ and temperature $T$              |
| $\tau = 1/k$                              | Generalised lifetime, a function of temperature $T$                                     |

## 1 Introduction

Change of scales for measurable observables is profitably employed for those sets of problems that require the dealing of properties involving large ranges of variation of quantities: they are often encountered for phenomena in nature and studied in laboratories, engineering, and materials science. In modern approaches, on the footsteps of the classical kinetic theory of gases, the systematic development of scaling and renormalization techniques permitted formulations of models at the foundation of theories, in order to transfer them up and down across micro-, meso-, macro-levels. As lucidly presented in (Weinberg 1995) (especially in Chapter 18), the procedures involve inevitably the costs and the benefits of the progressive reduction in the number of variables and effective degrees of freedom in descriptions preserving the essential features of the processes.

In the last decades, treatments of phase transitions lead to the discovery of classes of universalities beyond those well consolidated previously (Honig and Spalek 2018). Reference models set the gauge to calibrate renormalization by scaling, essentially providing a “theory of the theories”—with no claim of uniqueness but rather with perspective gain in insight and predictivity. The efficacy of parametrizations has to be assessed a posteriori.

In pure and applied chemistry, logarithmic scaling is familiar: the definitions of pH and pK for hydrogen ion concentrations and equilibrium constants involve reciprocals and logarithms of quantities. The development of chemical thermodynamics mapped reductions of the statistical–mechanical

properties of the components of a system, for example the chemical potentials and the partition functions, unto those of a simpler one: the condition is that sacrifice of details involves minimal loss of generality and accuracy. These ideas were applied with spectacular success in the high-energy context of elementary particle physics, beyond that of gaseous and condensed matter (Wilson 1971a, 1990; Kadanoff 2013); they did not circulate systematically for molecular processes in the so-called thermal energy range, and specifically in the field of chemical reaction kinetics: yet in perspective, applications look promising regarding in particular biochemical reactions and biophysical processes.

Along the lines of the earliest applications of the renormalization methods to several basic statistical–mechanical problems [see seminal papers (Di Castro and Jona-Lasinio 1969; Wilson 1971a, b)], it is important to extend concepts related to scale invariance and universality classes to the modern phenomenology of the kinetics of chemical reactions, with perspectives of usefulness under extreme conditions, where the reference standard, the Arrhenius formula for the temperature dependence of rates, is violated. The enormously diversified quantitative and qualitative experimental information on the kinetics of chemical reactions has been considered since the middle of the nineteenth century as a fundamental yet challenging branch of modern science (Laidler 1985; Stiller 1989; Gorban 2021). The developments, specifically awkward when quantum effects are under focus, in principle require the numerically demanding solutions of a large set of coupled-channel Schrödinger equation, or explicitly dedicated semi-classical techniques (De Fazio et al. 2006, 2011; Aquilanti et al. 2010).

Benchmark results for quantum mechanical converged rate constants as a function of temperature that we have been progressively made available (Aquilanti et al. 2012; Cavalli et al. 2014; De Fazio et al. 2016, 2019, 2020) provide the basis for formulation and implementation of the theoretical construction for a prototypical three-atom reaction. The effort in the present paper is to explore the arguable power of a heuristic approach: indeed, as soon as the number of atoms in a reactive process increases even from small to moderate, accurate numerical solutions in general become intractable, approximations must be introduced, and their reliability checked. Accordingly, in this work, we focus on scaling and renormalization formulations to assist in the identification of universalities in the kinetics of chemical reactions and to enforce the theoretical modelling by effective, physically motivated parametrizations.

Ample phenomenological evidence suggests that the rates of a variety of processes near “room” temperature slow down by cooling according to the Arrhenius prediction, but then decline faster until practically stopping. This classical behaviour, referred to as *super-Arrhenius*, involves acceleration of rates by heating higher than anticipated by Arrhenius formula. The opposite viewpoint is

needed in a predicting the *sub*-Arrhenius cases when quantum mechanics is operative, attenuating the decline by cooling and describing rather the approach to zero absolute temperature at a finite value, referred to as Wigner's limit (Wigner 1932; Takayanagi et al. 1987).

This especially challenging case has been tackled by a sequence of recent converged quantum–mechanical three-body scattering calculations (De Fazio et al. 2006, 2011, 2016, 2019, 2020; Aquilanti et al. 2012; Cavalli et al. 2014): they involve the elementary reactions of F atoms with H<sub>2</sub> and HD, and benchmark rate constants were obtained in a full temperature range, from ultracold to higher than thermal. The region of validity of the Arrhenius formula and the observed experimental deviations (Tizniti et al. 2014) were quantitatively accounted for theoretically. The search of parametrized equations that permit scaling and formulation of uniform analytic models for the kinetics of chemical change, involves rescaling of the transitivity function, first introduced in (Aquilanti et al. 2017; Carvalho-Silva et al. 2017), which provide a comprehensive framework to disentangle universal features and a smooth description of the transition between the Arrhenius and the quantum tunnelling regimes.

For the corresponding set of essentially two reactions, the second one evolving in two channels, apparent activation energies and transivities are considered for temperatures higher than 10 K, below which resonances and other quantum mechanical effects emerge (De Fazio et al. 2019, 2020): these features are studied in the given references, and only alluded to in the present work. The range, where reactivity is dominated by moderate quantum–mechanical tunnelling, is of relevance in cold environments and particularly in astrochemistry. Interest in these reactions continues regarding experiments. New kinetic measurements (Bedjanian 2021) although not covering the tunnelling regime, confirm our previous theoretical validation of experimentally available data.

A scheme of the paper follows: in the next section, we tackle the ever-increasing observational evidence of a variety of cases that deviate substantially from the Arrhenius behaviour, applying scaling and renormalization ideas to basic aspects of chemical kinetics. As suggested previously (Carvalho-Silva et al. 2020), theoretical treatments permit us to generate analytic models starting from formulations of the apparent activation energy, or its reciprocal, the transitivity function, transparently allowing identification and cataloguing classes of universal behaviour. A coupled set of two first-order equations defines renormalized functions and connects information between the temporal evolution and the temperature dependence of the composition of the molecular constituents that participate in a reactive process.

The transitivity analysis relevant to the *sub*-Arrhenius case is applied in the third section for the prototypical three-atom reactions of fluorine atoms with both H<sub>2</sub> and HD covering rate constants in the range from 10 to 350 K. Universal behaviour of the transitivity functions renormalized and dimensionless is unveiled as asymptotically tending to the Wigner limit. The physical meaning of parameters is assessed and their relationship with features of the potential surface exhibited. Final remarks and a summary conclude the paper. An Appendix reports notions and notations.

## 2 Rise and fall of rate processes at low and high temperatures

### 2.1 Scaling and renormalization

The extraordinary heuristic success of the 150-year-old Arrhenius formula in describing the temperature dependence of rate processes was consolidated by the accompanying modern theoretical interpretation and molecular dynamics simulation of microscopic processes as manifestation of collisional activation of molecules, macroscopically observed as a statistically averaged distribution of myriads of events (Laidler 1985; Stiller 1989). This concept continues to provide the cornerstone of present chemical kinetics: in this research area, the current practice involves the graphical representation of the scaled semi-logarithmic plot of either experimentally measured, else calculated, or variously estimated rate constants  $k$  against reciprocal absolute temperature, the *Arrhenius plane*:

$$\ln k(\beta) \text{ vs. } \beta, \quad (1)$$

where the identification

$$\beta = 1/k_B T. \quad (2)$$

establishes the relationship of the variable  $\beta$  with the reciprocal absolute temperature  $T$ , scaled by Boltzmann constant  $k_B$  in consistent units of measurement. As exemplarily plotted in Fig. 1, the graph represents from left to right the cooling of the system, and from right to left the performance of the process upon heating.

The important property of a graph of  $k(\beta)$  in the plane (1) is that a decaying linear behaviour of the logarithmically scaled rate as a function of  $\beta$  is taken as abiding the Arrhenius law

$$k(\beta) = A \exp(-\varepsilon^\ddagger/k_B T). \quad (3)$$

The temperature-independent parameter, here designated  $\varepsilon^\ddagger$ , is conveniently individuated as the activation energy taken as constant by Arrhenius and Eyring: the temperature-dependent generalisation is the apparent

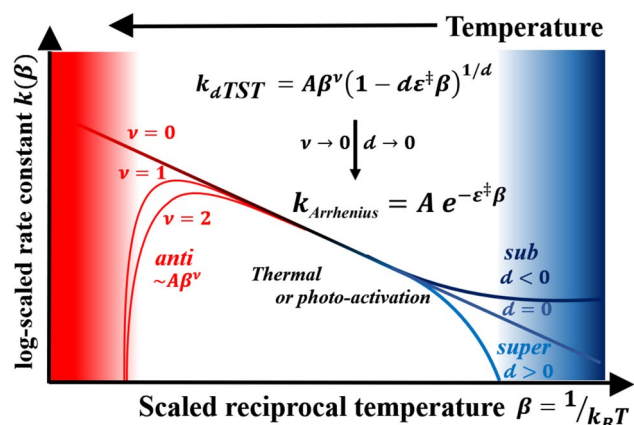


**Fig. 1** Ascent and decline of the rate constant  $k(\beta)$  by cooling or heating. The graphs in the  $k(\beta)$  vs  $\beta$  plane are here coloured to emphasise ubiquitous marginalisation of behaviour at extreme cold (blue) and hot (red) regions, the standard model is the deformed transition state theory,  $k_{dTST}$ . Illustrated are the deviations from linearity of the logarithmically scaled rate constant that occur in general and particularly for physicochemical processes: (i) in the low-temperature regime, where bifurcation occurs between quantum and classical (or respectively sub- and super-)Arrhenius regimes. (ii) At high temperatures, deviations are observed and the fall off is modelled by a power-like asymptotic parametrization by the exponent  $\nu$  (this embodies the so-called anti-Arrhenius behaviour). The case  $\nu = 0$  is considered in this work and denoted  $k_{AM}$ , see Appendix

“activation energy “  $E_a$ , operationally obtained by logarithmic differentiation of  $k(\beta)$  with respect to  $\beta$ :

$$E_a(\beta) \equiv -\frac{d}{d\beta} \ln k(\beta) = -\frac{1}{k(\beta)} \frac{dk(\beta)}{d\beta}. \quad (4)$$

This agrees with the definition recommended by the International Union for Pure and Applied Chemistry (IUPAC) (Laidler 1996). For any formula where  $k(\beta)$  is written in factored form like Eq. (3) or in Fig. 1, the pre-exponential factor or better the ‘prefactor’  $A$  that carries the units of measurement is independent of  $\beta$  and disappears by logarithmic differentiation.

This property of the logarithmic differentiation scaling (common in renormalization approach) compensates for any temperature-independent contribution embodied in  $A$ . According to the intuitive interpretation by Arrhenius, the macroscopic observable  $\varepsilon^\ddagger$  is an energetic barrier, namely an obstacle to reaction: the kinetic theory of gases microscopically correlated this potential energy to the kinetic energy that the reactant molecules must acquire for the reaction to start or to proceed to yield the products. The double dagger superscript ( $\ddagger$ ) is due to Eyring with reference to an assumed transition state of the reaction (Glassstone et al. 1941).

Deviations from linearities of the  $k(\beta)$  vs  $\beta$  plot manifest as a rule rather than exceptions at extreme either low or high

temperatures that confine the range of performance of the processes. At low temperature, convex or concave cases of curvature are designated as belonging to the *sub*-Arrhenius or *super*-Arrhenius behaviour, respectively corresponding to a temperature dependence that involves either higher or lower reactivity upon cooling (Aquilanti et al. 2017; Carvalho-Silva et al. 2017; Coutinho et al. 2018): reference to this behaviour expected from the Arrhenius formula. Decline in reactivity (the *anti*-Arrhenius behaviour) occurs eventually at temperatures higher than thermal, widely documented in radical–radical or ion–molecule reactions. This case is only briefly mentioned here but is extensively alluded to elsewhere (Coutinho et al. 2015, 2016; Sanches-Neto et al. 2021), it occurs as universal behaviour in biophysical processes and biochemical reactions (Arroyo et al. 2022; Guberman-Pfeffer 2022) as temperature increases.

The reaction rate constant expression of the variant of Transition State theory (*d* TST) (Fig. 1) is compacted introducing both the parameters  $\nu$  and  $d$  that encode the deviations at high and low temperatures (Carvalho-Silva et al. 2017), respectively. See Sect. 2.4 and in particular the Appendix for the notations.

A classical derivation due to Tolman (Tolman 1920, 1927) and generalised to quantum mechanics by Fowler and Guggenheim in their treatise on Statistical Thermodynamics (Fowler and Guggenheim 1939) provides an interpretation for the function  $E_a$  [Eq. (4)] as the difference between the average over the kinetic energy of all reacting particles in the system and that of all particles, both reactive and nonreactive. Therefore, Eq. (4) establishes the key role of  $E_a$  as a coupling function in the presently enforced renormalization procedure of the rate constant and propitiates a connexion between canonical quantities with microcanonical features. The association of parameters from a renormalization procedure to those of the potential energy surface upon which the process is supposed to adiabatically evolve, is resumed in (Aquilanti et al. 2018) and amplified here with respect to the presentation of the *alpha–zeta* totem in (Carvalho-Silva et al. 2020).

It has been recently demonstrated as crucial to the theory to introduce the reciprocal of the apparent activation energy (Carvalho-Silva et al. 2019, 2020)

$$\gamma(\beta) \equiv \frac{1}{E_a(\beta)} = -k(\beta) \frac{d\beta}{k(\beta)}. \quad (5)$$

This differential equation defines the transitivity function  $\gamma(\beta)$  (Carvalho-Silva et al. 2019, 2020; Machado et al. 2019). Remarkable is a formal similarity between the functional form of this definition involving the reciprocal of a logarithmic differentiation and the Callan–Symanzik (Callan 1970; Symanzik 1971) function occurring as the renormalization group order parameter, which encodes

the mathematical apparatus of statistical field theories (Parisi 1998), and permits handling of singularities in the treatment of critical phenomena.

In a chemical kinetics scenario, the temperature  $T$  or its scaled reciprocal  $\beta$  play the part of the control parameter, whilst the role of the coupling is provided by the rate constant  $k(\beta)$ . Conversely, let us consider as usual its reciprocal  $\tau(\beta)$  defined as follows and designated as the *generalised lifetime* of the process

$$\tau(\beta) \equiv \frac{1}{k(\beta)}. \quad (6)$$

It is the renormalization though Eq. (5) that permits a substantial advance for the interpretation of the dynamics of chemical reactions and motivates the construction of an appropriate scaling transitivity plane,

$$\gamma(\beta) \text{ vs. } \beta \quad (7a)$$

The deviation from constancy of the transitivity as a function of temperature is graphically emphasised: according to Eq. (5).  $\gamma(\beta)$  can be interpreted as the function that measures the propensity for the reaction to proceed. It permits us to uniformly account for experimental and theoretical important features in rate processes, intrinsic of the reacting system. They include quantum mechanical tunnelling and the effects on transport properties in neighbourhoods of changes in chemical kinetics mechanisms: these enforce continuities excluding apparent breaks occurring at sudden regime changes (Carvalho-Silva et al. 2020).

As already remarked (Carvalho-Silva et al. 2019, 2020), the plot in the transitivity plane, Eq. (7a), enjoys the features that deviations from Arrhenius behaviour can be given a geometrical representation by the deformation parameter  $d$  as the arc measuring the angular slope  $\delta$  of  $k(\beta)$  as  $\beta$  varies as [see Fig. 1 in (Carvalho-Silva et al. 2019) and Eq. (18b) in SubSect. 2.3]

$$d = -\tan \delta \quad (7b)$$

This parametrization is important for transition from the Arrhenius to quantum tunnelling regime: it makes explicit the bifurcation to the *super-* and *sub-*Arrhenius propensities according to whether  $d$  is respectively positive or negative. In the latter case, of particular relevance in this paper, it is directly correlated with quantum mechanical tunnelling, and explicit formulas involving the curvature transversal to the reaction profile were derived, implemented and tested in (Aquilanti et al. 2012).

## 2.2 Time dependence of rate processes: the mechanism

For handling expressions for rates describing dependences of compositions of systems occurring either in experiments or in modelling, we consider effective reformulations from the mass action law as initially systematised according to the famous van't Hoff book in 1884 (van't Hoff 1884): see recent developments (Laidler 1985; Gorban 2021).

This is also expedient to consider the concept of rate constant and activation energy as function not only of temperature but also of time, as discussed in various contexts (Vyazovkin 2016; Piskulich et al. 2019; Rufino and Guedes 2022).

Formally, let's write as usual a general chemical reaction as a transformation between left- and right-hand sides of the formally balanced "equation":



where  $[A]$ ,  $[B]$ ,  $\dots$  are a measure of compositions of reacting species with stoichiometric coefficients  $a$ ,  $b$ ,  $\dots$  (counterparts for one of products are  $[C]$  and  $c$ ). An inherent ambiguity of balancing chemical equations is that for example (8) can be multiplied or divided by any number, so that the set of stoichiometric coefficients is defined *modulo* this number. An ad hoc, admittedly partial, disambiguation is here attempted by a renormalizing standardisation.

As time evolves, the progressive conversion of chemical species  $A$ ,  $B$ ,  $\dots$  (the "reactants") into  $C$ ,  $\dots$  (the "products") under idealised conditions occurs with the rate,

$$-\frac{1}{a} \frac{d}{dt}[A] = -\frac{1}{b} \frac{d}{dt}[B] = \frac{1}{c} \frac{d}{dt}[C] = \dots \quad (9)$$

The practice of chemistry, as evolved after the statement of the "law of mass action" (Laidler 1985; Gorban 2021) thus involves the description of a system as a *field* of the system containing the  $A$ ,  $B$ ,  $C$ , species as a function of time and temperature.

It is often operationally attempted, especially in chemical engineering or in industrial chemistry, to focus on compactly one reagent only, say  $R$ , that is generally decreasing. If this is possible, we denote the corresponding renormalized stoichiometric coefficient by  $\rho$ , to be interpreted as the *generalised reaction order*, also designated as the *pseudomolecularity*. If one instead of following the reagent  $R$ , finds it practical to monitor experimentally or to simulate in molecular dynamics a representative product

increasing progressively in time, formally the stoichiometry should provide a connexion. This procedure requires the knowledge of independent information, or as stated commonly, some knowledge of the reaction “mechanism”.

The effective compositions for the system under study should be ideally followed for each species, as a measure of either experimentally the involved macroscopic mass, or else in simulations the microscopic number of particles in a given volume. The units of measurements can be those of partial pressures, concentrations in solution, fugacities, activities: these alternatives and the connexions between them were canonised principally according to the 1922 treatise Lewis–Randall (Lewis and Randall 1922).

In this view, a heterogenous process is considered as a homogeneous system, where activities of components of different phases do not appear explicitly, because they are assumed in equilibrium and therefore with the activity value 1 of the standard state at that temperature. In practice, let's assume as operationally in a reaction kinetics experiment, the instantaneous measurements of  $R$  in progressive intervals of times as performed on a temporal grid spacing much greater than the estimated “time scale”  $\tau$  of the process: then, one may implicitly enforce a thermodynamic macrocanonical description of the time dependence of the mixture as it nearly equilibrated at key intermediated steps, in particular at the transition state.

By focussing on a reactant  $R$ , one enunciates that it exists a function of  $\beta$ , the rate coefficient  $\hat{k}(\beta, t)$  of the reaction (and its reciprocal  $\hat{\tau}$ ) that is defined from the time change of  $\hat{R}$ , the cap making explicit the time-dependence functionality:

$$-\frac{\partial}{\partial t}[\hat{R}(t, \beta)] = \hat{k}(t, \beta)[\hat{R}^\rho(t, \beta)] \quad (10)$$

This operational enunciation of the existence of  $\hat{k}$  is not free from ambiguities: to be implemented, it must be flexibly adapted with respect to the external conditions into which the process is embedded, in general the reaction “mechanism”.

The interpretation and the use of this and following equations need also explicit operational definitions, and specification of the experimental configuration, for example whether the reaction takes place in a closed system [the “reactor” Astarita and Ocone 1988, 1990; Astarita 1989] or in an open environment, such as in atmospheric or combustion processes (Adam et al. 2012). Equation (10) embodies the role of the ambient on the system and permits us to establish an extrinsic renormalized rate constant  $\hat{k}$ , which according to the chosen presentation can be compacted by the observation of only the single reactant  $R$  as a monitor.

In general, the above references show that a variety of different situations may occur, specifically in a chemical industrial or pharmaceutical plant, in geochemistry, in flames or in atmospheric chemistry implementations, or even in a

biological cell: see (Kummer and Ocone 2005) and references therein. Often, the terminology of chemical kinetics is employed, compacting (lumping) a complicate process as described by the representative reagent  $R$ ; then  $\rho$  as in Eq. (10) is a heuristic reaction order parameter that we allow to be possibly non-integer and even continuous but typically a small number.

In favourable cases, when sets of data on time evolution are available on more than one reagent or more than one product, the practice of chemical reaction mechanisms suggests to profitably exploit the augmented information to increase the accuracy of parametrizations. An example is given in (Nishiyama et al. 2009a, b), where in a study on respiration kinetics of leaves, the configuration of the reactor is a closed volume vessel, and both decrease in reactant  $O_2$  and simultaneous increase in product  $CO_2$  were accurately monitored. The observed *super-Arrhenius* process was constrained as pseudo-unimolecular, namely in the present context assigning the value  $\rho = 1$ .

### 2.3 A set of coupled renormalization equations and their decoupling

In order to encode information both on the temporal evolution and on the temperature dependence of the composition of the molecular constituents participating in a reactive process, here we formulate a system of coupled set of differential equations that provide an explicit reference framework for renormalization in chemical kinetics.

Considering time  $t$  as a running variable, and assigning the role of the order variable to the properly rescaled absolute temperature  $T$  or its reciprocal  $\beta$ , the field of matter transformations (Weinberg 1995) of interest in chemical reaction kinetics can be written as the function designated by  $\hat{R}(t, \beta, k)$ , that obeys Eq. (10). This equation compacts the experimental and the empirical available data on the compositions. Then, let's formulate that the following coupled set of two partial differential equations represents a concrete coupling scheme, transcribed by rearranging Eqs. (5) and (10) (the dependence on the  $\rho$  order parameter is omitted from the notation for  $\hat{R}$  and  $\hat{k}$ ),

$$-\frac{\partial}{\partial t} \ln[\hat{R}(t, \beta)] = \hat{k}(t, \beta) [\hat{R}(t, \beta)]^{\rho-1}, \quad (11)$$

$$-\frac{\partial}{\partial \beta} \ln \hat{k}(t, \beta) = \frac{1}{\hat{\gamma}(t, \beta)}. \quad (12)$$

The first Eq. (11) is a generalisation of the mass action law introduced by van't Hoff in chemical kinetics: it is twinned to the second one (12) that generalises the validity range of Arrhenius law through the transitivity function  $\hat{\gamma}$ , that we momentarily consider as time-dependent.

Exploiting transformations of variables, we may have formulated equivalent coupled systems writing the first equation as a function of temperature  $T$  instead of  $\beta$  [Eq. (2)], and the time dependence of rate constant  $\hat{k}(\beta, t)$ , namely the parameter controlling the coupling, introducing its reciprocal

$$\hat{\tau}(\beta, t) = \frac{1}{\hat{k}(\beta, t)}, \tag{13}$$

the *generalised lifetime* of the process or its time constant.

As a practical scheme, Eqs. (11) and (12) are operationally applied “instantaneously”, from the neighbourhood of an initial time,  $t \approx 0$ , when the “clock” is started experimentally, or simulations are initiated computationally. Then, when  $t \rightarrow 0$ , the caps are eliminated from the notation and one can turn the coupled set to look like a renormalization set of two uncoupled ordinary differential equations, explicitly

$$-[\mathbf{R}(t)] \frac{dt}{d\mathbf{R}(t)} = \frac{1}{k(\beta)} [\mathbf{R}(t)]^{1-\rho}, \tag{14}$$

$$-k(\beta) \frac{d\beta}{dk(\beta)} = \gamma(\beta), \tag{15}$$

This set involving reciprocals of logarithmic differentiation has to be regarded as similar to (and playing an analogous fundamental role of) the reciprocal of logarithmic differentiation in Sec. 12.4 of (Weinberg 1995) and in Eq. (9) of (Wilson 1971a).

Useful is the property that these equations can be written in alternative equivalent coupling schemes by convenient change of notations for key quantities explicitly defined, for example in terms of their reciprocals and/or opposites. The procedure permits a variety of applications. One can enforce robust models, either for the dependence only on the temperature of  $\tau$  or  $k$ , and also of  $E_a$  or  $\gamma$ , but not from time. This gives to the apparent activation energy and the transitivity function in Eq. (15) the feature of an intrinsic characterisation of the reacting system.

Important is to exploit the extrapolation of  $\hat{k}$  in the limit of  $t \rightarrow 0$ , that enables a general solution to Eq. (14) as a one-dimensional integral: when complemented by boundary conditions dictated by features of the “reactor”. Typically, at a given initial time  $t=0$  in a closed volume, let  $[\mathbf{R}]$  be  $[\mathbf{R}]_0$ . Then, the solution of (14) is

$$[\mathbf{R}(t)] = [\mathbf{R}]_0 \left[ 1 - (1 - \rho)k(\beta)[\mathbf{R}]_0^{\rho-1}t \right]^{1/1-\rho}; \quad \forall \rho \neq 1 \tag{16a}$$

when  $\rho = 1$ , the apparent singularity disappears through the Euler’s limit, and the common case occurs of the typical exponential decay of first-order or *pseudounimolecular* kinetics

$$[\mathbf{R}(t)] = [\mathbf{R}]_0 e^{-kt}, \tag{16b}$$

in this case,  $\tau = 1/k(\beta)$  is considered as the time constant of the system in consistent units of  $\text{time}^{-1}$ .

The freedom of choosing alternative representations in some quantities like their reciprocals, can be syncretically exploited as alternative coupling schemes, up advantage specifically in perturbation formulations or as more convergent basis set in computational approaches. A cautionary remark is in order. In practice, the equations in this section have much more than only a formal character and are ubiquitously used, although not in this form in chemical kinetics: however, one-to-one correspondence with observables needs consideration, such as dependence on scaling to express the field function  $[\mathbf{R}]$  in alternative composition units. Note that the treatment and the parametrization of the coupled set may serve both to provide models from measured quantities, and also conversely to physically substantiate theoretical parameters in order to predict time and temperature dependence of the observables of rate processes.

### 2.4 General models for transivities and the transition between thermal and sub-Arrhenius regimes

To be considered next are recent systematic investigations leading to formulations of models to be inserted in Eq. (15) involving transivities, and the temperature dependence of apparent activation energies. We argue that it is expedient to use the already encountered dimensionless deformation parameter  $d$  to describe low-temperature deviation from Arrhenius behaviour. The  $d$ -Arrhenius, also known as the Aquilanti–Mundim formula, was obtained (Aquilanti et al. 2010) by extending the Tsallis non-extensive statistical–mechanics (Tsallis 2009) to the quantum tunnelling case. One exploits Euler’s expression of the exponential function as the limit of a succession. This in previous work was documented as crucial for monitoring how close a system to reach the thermodynamic limit, see Appendix and Refs. (Carvalho-Silva et al. 2019, 2020). In Fig. 1, the general  $d$  TST formula is written

$$k_{dTST}(\beta) \equiv A\beta^\nu (1-d\epsilon^\ddagger \beta)^{1/d} \tag{17a}$$

and the quantum tunnelling case corresponding to  $d < 0$ . Equation (17a) implies for  $\nu = 0$  the Aquilanti–Mundim formula

$$k_{AM}(\beta) \equiv A(1-d\epsilon^\ddagger \beta)^{1/d} \tag{17b}$$

The expression for the rate formula Eq. (17a) was derived in (Carvalho-Silva et al. 2017). It is here compacted introducing the parameter  $\nu$  additionally to  $d$ : they encode the deviations from Arrhenius law at high and low temperatures, respectively. In the following, since for this system there is no evidence of high temperature deviation from Arrhenius in the studied range, we take  $\nu = 0$ , pertinent to the range of thermal and low temperatures here investigated.

In (Carvalho-Silva et al. 2019, 2020; Machado et al. 2019), an analytical form was proposed and implemented for the transitivity beyond the Aquilanti–Mundim (AM) formula

$$\gamma(\beta; \zeta) = \frac{1}{\varepsilon^\ddagger} (1 - \varepsilon^\ddagger \beta)^\zeta \quad (18a)$$

where for the AM case ( $\zeta = 1$ ), the identification holds

$$\varepsilon^\ddagger = d\varepsilon^\ddagger = k_B T^\ddagger. \quad (18b)$$

Equation (18a) condenses the generic temperature dependence at low temperatures, as extensively exemplified in the above references. In the classical propensity case, the parameter  $\varepsilon^\ddagger$  is the energy that upon cooling marks the minimal energy for survival, whilst upon heating, it marks the onset energy for the process to start performing (this concept is arguably of interest in biological systems, see for example (Consolini et al. 1992; Carrà 2021)). Therefore, in the classical case, it may serve to elucidate the meaning of the energy term  $\varepsilon^\ddagger$  and temperature  $T^\ddagger$ , which for the quantum case needs particular scrutiny: it can be shown at face value that both should be negative, according to the negative sign of  $d$  for the quantum mechanical tunnelling regime. Then, the  $\varepsilon^\ddagger$  energy parameter (and  $T^\ddagger$  through 18b) can be interestingly connected to the imaginary frequency mode of the transition state: this has been previously investigated explicitly in (Silva et al. 2013; Cavalli et al. 2014; Carvalho-Silva et al. 2017), where robust models of quantum mechanical tunnelling were implemented and tested for the processes considered in the next section.

The general model for transitivity Eq. (18a) permits by direct rearrangement to propose a dimensionless *renormalization plane*

$$(\varepsilon^\ddagger \gamma)^{1/\zeta} \quad \text{vs} \quad 1 - \varepsilon^\ddagger \beta. \quad (18c)$$

to be tested in the next section for the *sub*-Arrhenius case, and to be compared with the two cases  $\gamma$  vs  $\beta$  presented in (Carvalho-Silva et al. 2019) (Fig. 2) and distinguishing the behaviour for  $d > 0$  and  $d < 0$ .

Then, the expression for  $\gamma$  on Eq. (18a) can be obtained as a general formula for the temperature dependence of the

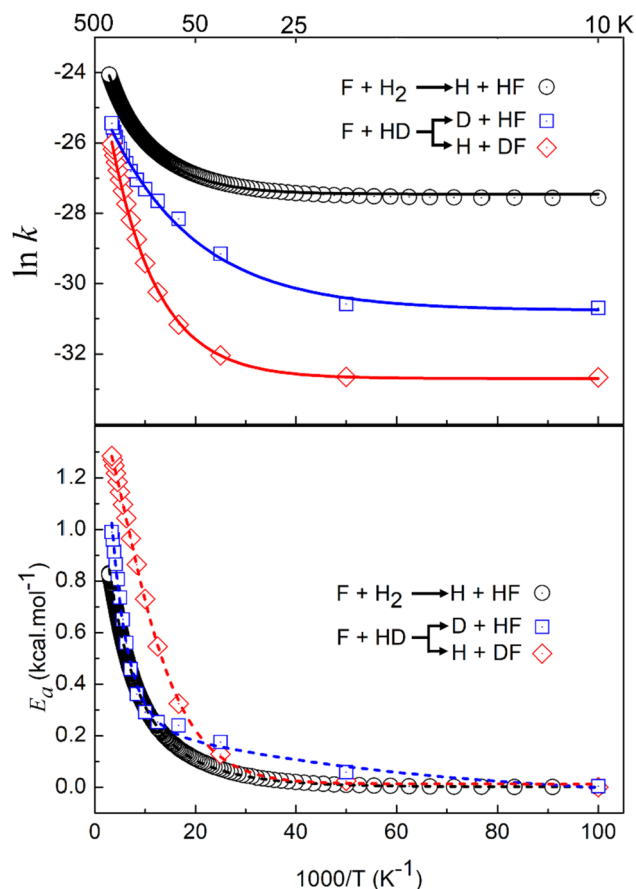


**Fig. 2** Arrhenius plots and Activation energies for the  $F+H_2$  reaction and its isotopic variant producing  $HF+D$  and  $DF+H$ .  $E_a(\beta)$  is calculated as the negative of the numerical logarithmic derivatives of rate constants with respect to the reciprocal of absolute temperature  $T$ . Continuous lines in the upper panel are result of the final fit (parameters in bold in Table 1). In the lower panel, as well as in Fig. 3, broken lines are aid to the view. Trends of converging behaviour is qualitatively shown and quantitatively assessed numerically, confirming the results for  $\varepsilon^\ddagger$  in Table 1

reaction rate constant. Inserting Eq. (18a) in Eq. (5) and considering the integral

$$\ln k(\beta; \zeta) = - \int \frac{d\beta}{\gamma(\beta; \zeta)} + const \quad (19a)$$

the identification of the constant with the logarithm of the prefactor gives the Carvalho–Coutinho–Aquilanti (CCA) formula

$$k_{CCA}(\beta; \zeta) = A \exp \left[ - \frac{1}{(\zeta - 1)} \frac{\varepsilon^\ddagger}{\varepsilon^\ddagger} (1 - \varepsilon^\ddagger \beta)^{1-\zeta} \right], \quad (19b)$$

that when the exponent  $\zeta$  tends to 0, 1, and 2 generates the Arrhenius, Aquilanti–Mundim (AM), and Vogel–Fulcher–Tammann (VFT) laws, respectively, see also (Carvalho-Silva et al. 2019, 2020).

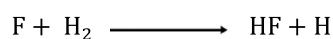


Detailed derivation of (19b) involves Eulerian integrals and hypergeometric functions. For the uniform covering of the high-energy behaviour, the treatment for the passage between the *anti*-Arrhenius case and the thermal regime (Carvalho-Silva et al. 2020) involves a Confluent Hypergeometric Function, explicitly an Incomplete Gamma Function (Abramowitz and Stegun 1965). Further, using a Gaussian Hypergeometric Function, explicitly an Incomplete Beta Function (Abramowitz and Stegun 1965), the formulation is possible to cover both high- and low-regime changes illustrated in Fig. 1. This will be documented elsewhere.

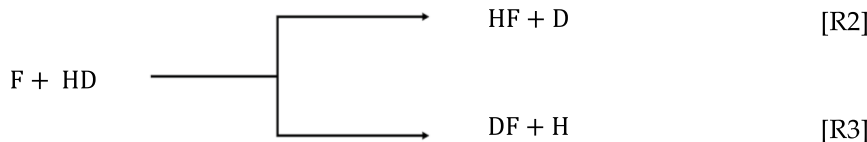
### 3 An elementary chemical reaction as a complex system

#### 3.1 Converged results for the kinetics of the F + H<sub>2</sub> (HD) reactions

As prototypical of the Arrhenius vs *sub* case transition, explicit focus will be devoted next to applying the transitivity-based approach of the previous sections to two reactions of fluorine atoms, one with hydrogen molecules leading to hydrogen fluoride,



and the other with HD leading to both HF + D and DF + H.



The search of universality of behaviour is illustrated for the moderate tunnelling range including that of validity of the Arrhenius law and excluding that of quantum mechanical resonances towards the Wigner limit at zero Kelvin.

The rate constants for the F + H<sub>2</sub> reaction and its isotopic variants have aroused great attention from experimental and theoretical chemical kinetics studies (Aquilanti et al. 2005b; Cavalli et al. 2014; Tizniti et al. 2014; De Fazio et al. 2019). These processes are prototypical of exothermic elementary reactions driven by the quantum tunnelling effect even at room temperature, becoming dominant in the colder environments. In the present demonstrative simulations of the renormalization approach, we take at face value selected data from calculations from (Aquilanti et al. 2012) for R1 and from (De Fazio et al. 2016) for R2 and R3. The numerically converged results included all open roto-vibrational

levels of products. R1 is studied on PES I, a variant of the early Stark–Werner potential energy surface (Stark and Werner 1996; Aquilanti et al. 2012), extensively modified afterwards. The much harder case of HD, carried out later (Cavalli et al. 2014) employed a more recent surface denoted FXZ (Fu et al. 2008).

These reactions are written as elementary chemical reactions, but are actually case studies of complex systems. (Cavalli et al. 2014) and (De Fazio et al. 2019) provide additional detailed insights coming from rigorous quantum scattering calculations carried out for rate constants  $k(T)$  and including the temperature dependence on alternative potential energy surfaces. All results confirm a linear asymptotic behaviour in Arrhenius plots at high temperature, whilst ubiquitous concave curvature was observed at low temperature. This is a manifestation of the insurgence of *sub*-Arrhenius behaviour, as macroscopic evidence of quantum mechanical tunnel of H atoms in R1 and R2 or D atoms in R3, to be looked at next from the viewpoint of this paper.

#### 3.2 Renormalization across the thermal and the sub-Arrhenius regimes

The data selected from 10 to 350 K for the reaction constants and those calculated for the temperature dependence

[R1]

HF + D [R2]

DF + H [R3]

of activation energies and transivities are presented in the next figures. Available data at lower energies fall in the quantum mechanical resonance region extensively investigated elsewhere (Aquilanti et al. 2004, 2005a; Sokolovski et al. 2007). Activation energies and Transivities defined in Eq. (5) are obtained numerically by logarithmic differentiation of the reaction rate constants with respect to  $\beta$ , Eq. (2). Having to deal with experimental or theoretically concrete systems, notations will be specialised somewhat in this section with respect to previous ones. Specifically,  $\beta$  will be given in  $1000/T$  units for Arrhenius and Activation Energy plots and consequently inverse units for the plots of Transivities. This was the initial step of the approach was to assign the energy parameter  $\epsilon^\ddagger$  (see Refs. Aquilanti et al. 2012; De Fazio et al. 2016) to be intended as the Arrhenius–Eyring barrier to reaction, arguably similar for

**Table 1** Kinetic parameters obtained fitting data for F + H<sub>2</sub> and HD reactions<sup>a</sup>

| Reaction                    | A               | $\epsilon^\ddagger(\text{kcal.mol}^{-1})$ | $\epsilon^\ddagger(\text{kcal.mol}^{-1})$ | $\zeta$     | Refs for $k(\beta)$                        |
|-----------------------------|-----------------|---|---|-------------|--|
| F + H <sub>2</sub> → HF + H | –               | 1.54                                      | – 0.048                                   | 6.0         | Using PES I in Aquilanti et al. (2012)     |
|                             | –               | 1.24                                      | – 0.048                                   | 6.2         |  |
|                             | <b>1.01E-12</b> | <b>1.33</b>                               | <b>– 0.077</b>                            | 4.4         |  |
|                             | 2.48E-12        | 1.22                                      | – 0.204                                   | 1.0         | Aquilanti et al. (2010)                    |
| F + HD → HF + D             | –               | 1.60                                      | – 0.034                                   | 4.0         | Using PES FXZPES in De Fazio et al. (2016) |
|                             | –               | 1.12                                      | – 0.024                                   | 3.6         |  |
|                             | <b>3.87E-14</b> | <b>0.79</b>                               | <b>– 0.021</b>                            | <b>6.9</b>  |  |
|                             | 2.56E-11        | 1.22                                      | – 0.586                                   | 1.0         | Cavalli et al. (2014)                      |
| F + HD → DF + H             | –               | 1.56                                      | – 0.012                                   | 9.1         | Using PES FXZPES in De Fazio et al. (2016) |
|                             | –               | 1.90                                      | – 0.007                                   | 15.0        |  |
|                             | <b>6.10E-15</b> | <b>1.11</b>                               | <b>– 0.007</b>                            | <b>17.0</b> |  |
|                             | 5.16E-11        | 1.58                                      | – 0.158                                   | 1.0         | Cavalli et al. (2014)                      |

<sup>a</sup>The first lines in each channel are parameters obtained from fitting rate constants by Eq. (18a) for F + H<sub>2</sub> → HF + H reaction and its isotopic variants keeping  $\epsilon^\ddagger$  fixed at the energetic barrier calculated from the PES. Second lines, all parameters, except A, were obtained by fits from Eq. (18a). Third lines, in bold, all parameters including the prefactor A are obtained fitting rate constants by Eq. (19). Fourth lines, parameters from fits with the Aquilanti-Mundim formula, Eq. (17b), that assumes  $\zeta = 1$ . Units cm<sup>3</sup>.molec<sup>-1</sup>.s<sup>-1</sup>.

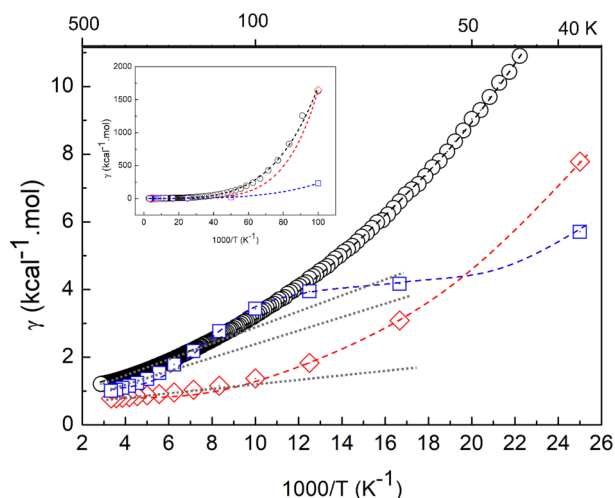


**Fig. 3** Transitivity function  $\gamma$  as a function of reciprocal of temperature for the studied reactions, symbols as in Fig. 2, obtained from quantum scattering reaction rate constants of Refs. (Aquilanti et al. 2012; De Fazio et al. 2016). The inset shows the general trend. Blown up is the transition temperature range across the thermal and moderate tunnelling regimes where broken lines indicate the trends to linearization leading to parametrization through the Aquilanti-Mundim formula

the three cases. For these systems,  $\epsilon^\ddagger$  and  $\zeta$  are fitted from Eq. (18a) on the transitivity data, to be discussed below, but the temperature dependence was poor.

Figure 2 shows Arrhenius (top) and Activation energies (bottom) plots for the F + H<sub>2</sub> reaction and its isotopic variant with HD producing HF + D and DF + H. In all cases, a decrease of activation energies was observed as temperature decreases. This behaviour of the apparent activation energy had been already reported in the previous paper (Aquilanti

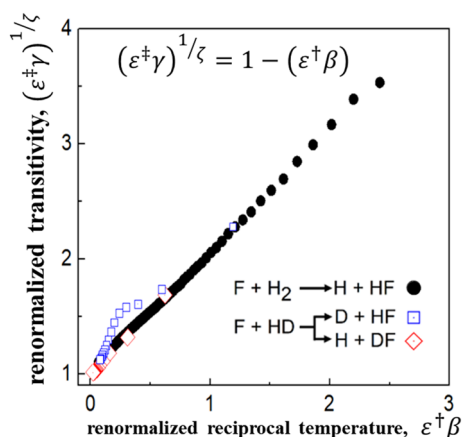
et al. 2012) for the first reaction only. Their scrutiny makes the search of universalities of behaviour easier to be captured visually: convergence to similar trend for  $\beta = 0$  is observed (Fig. 2) as for the reasonably common initial guess. Indeed, numerical search involving extrapolation of  $E_a(\beta)$  towards  $\beta = 0$  confirms the results for  $\epsilon^\ddagger$  in the three cases and listed in Table 1 in units of kcal.mol<sup>-1</sup>. On taking into account that in theoretical chemistry conventionally “chemical accuracy” is considered tolerable within 1 kcal.mol<sup>-1</sup> and “spectroscopical” data are accepted as reliable within a 0.10 kcal.mol<sup>-1</sup> accuracy, we can affirm that the four values (Table 1) indicate essentially the same height of the derived effective barrier energy  $\epsilon^\ddagger$  for the reactions to proceed.

Figure 3 presents the plots of the Transitivity function for the three cases. Upon cooling, *i.e.* when  $\beta$  increases, transivities grow indefinitely according to a trend to be expected from exothermic tunnelling (Takayanagi et al. 1987; Carvalho-Silva et al. 2019) and to be compared to that of the proposed model relationship in the Eq. (18a). Remarkably, Refs. (Silva et al. 2013; Carvalho-Silva et al. 2017, 2019) advocate the relevant property of the transitivity function to behave linearly in the small  $\beta$  limit for processes that deviate from the Arrhenius formula according to the Aquilanti-Mundim (Aquilanti et al. 2010) formula, and implemented in the *deformed* Transition State Theory (*d* TST) (Carvalho-Silva et al. 2017). Calculations applying the *d* TST for chemical reactions upon the potential energy quantum chemical calculated surface profile have been reported for a variety of processes, such as the CH<sub>4</sub> + OH (Carvalho-Silva et al. 2017), CH<sub>3</sub>OH + H (Sanches-Neto et al. 2017), OH + HCl (Coutinho et al. 2018) reactions, the proton rearrangement of enol forms of curcumin (Santin et al. 2016), the degradation of a pesticide (Sanches-Neto et al. 2021),

and the Claisen–Schmidt condensation (Coutinho et al. 2021), all involving deviations from Arrhenius because of quantum mechanical tunnel.

The scaling plane exhibits the transitivity function, which allows the estimation of potential energy surface parameters whilst avoiding the kinetic compensation effect (Garn 1975; Zuniga-Hansen et al. 2018). For systems that exhibit a well-behaved trend, such as the one shown for reaction R1 in Fig. 3, the model given by Eq. (18a) fits perfectly. Table 1 presents a comparison of fits made on Arrhenius (Fig. 1) and transitivity planes (Fig. 3). In Table 1, the first three lines list parameters in this work whereby fit improved by letting  $\zeta$  varying additional to  $\varepsilon^\ddagger$ . In the fourth line of each system, the parameters from previous fit using the  $k_{AM}$  formula corresponding to  $\zeta = 1$ . For each reaction, an initial fit of the temperature dependence of transitivity was performed using Eq. (18a) in the range of 10–350 K. As a first step,  $\varepsilon^\ddagger$  was kept constant and equal to the energetic barrier obtained by electronic structure calculations in the references cited in the table; in a second step, the fit is performed without restrictions. In the third case for each reaction, from the temperature dependence for the reaction rate constant, a fit was also performed using the general model proposed in Eq. (19a, 19b), inserting the pre-factor as an additional variable to be obtained.

The third case is compared with fits made previously in a temperature range where the linear model of transitivity is appropriated and described by the Aquilanti–Mundim formula. In both cases, the energetic barriers present values consistent with calculations obtained through electronic structure methods, considering that differences do not exceed error limits of  $1 \text{ kcal.mol}^{-1}$ . Additionally, energetic barriers obtained by electronic structure calculations ignore dynamic effects embedded in reaction rate constant



**Fig. 4** Universal behaviour of the transitivity functions  $\gamma(\beta)$  renormalized according to Eq. (18a) for the reactions R1, R2 and R3, symbols as Figs. 2 and 3. Parameters are listed in Table 1

calculations and emphasised here by scaling and renormalization methods.

The transitivity at cold and ultracold temperature sharply increases according to the universality class measured by the  $\zeta$  parameter, and balances the loss of active number of particles with decreasing temperature. This results in the finite Wigner limit at zero kelvin.

Rearrangement of Eq. (18a) (Eq. 18c and Fig. 4) in terms of rescaled dimensionless variables  $\varepsilon^\ddagger \gamma$  and  $\varepsilon^\ddagger \beta$  collapses in a universal behaviour (see fitting data in Table 1). A linear relationship is found for the three reactions in the limit of low temperatures where the passage from the room temperature regime to that of quantum mechanical tunnelling occurs. Remarkable is the diagnostic that indicates as anomalous the deviation from linearity observed for  $F + HD \rightarrow HF + D$  at intermediate temperatures, although at low temperatures, linearity is recovered. This anomaly may be ascribed to previously observed insurgent quantum resonances (De Fazio et al. 2020) at low temperatures. Open is the interesting perspective of further investigation along this direction for these systems at higher energies to study the transition across the Arrhenius vs anti-case regimes. This is in a region of temperature very demanding for exact converged calculations, especially for the R3 channel that requires including a very high roto-vibrational density of states of the product.

## 4 Conclusions and perspective remarks

In retrospect, renormalized formulations widely used in the physics of critical phenomena and of elementary particles, have been here exemplarily applied to the kinetics of elementary chemical reactions. In the thermal and low-temperature regimes, this study of the  $F + H_2$  (HD) reaction provides accurate information on the temperature dependence of the quantum mechanical benchmark rate constants, permitting a reliable opportunity to applying the renormalization approach at the transition across the Arrhenius and the sub-Arrhenius cases. The notations for atoms and molecules in the previous sections and specifically in R1, R2 and R3 above hide the complexity of many-electron atoms and molecules limiting to their bound states, and deal basically on average properties, in the case of F by treating adiabatically the fine structure due to the spin–orbit interaction (Aquilanti et al. 1990, 2001b), in the case of  $H_2$  by averaging through nuclear isotopic statistics. The kinetic energy and the roto-vibrational manifold were Boltzmann-convoluted at the given temperature. For computational overcoming of convergence problems, see (Aquilanti et al. 1998, 2001a), and for complexities from steric, isotopic and state-to-state dynamics, see (De Fazio et al. 2006, 2008; Skouteris et al. 2009). Renormalization by the transitivity function is enforced by

Eqs. (18a) and (18c), which compact by a uniform description, the behaviour of processes at low temperatures.

The plot in Fig. 1 illustrates the chemical kinetics and expands the previous ones in (Fig. 2) of (Carvalho-Silva et al. 2019, 2020) to cover both rise and fall as a function of temperature of the performances of processes for diverse models that operate at widely differing scale ranges. Prime interest is for chemical and biophysical processes upon cooling or heating. Enormous changes in the orders of magnitudes are involved in materials sciences, and in geochemistry at the largest of scales. It is even tempting to conceive a cosmochemical toy model for the molecular evolution of the universe, as it had been cooling down from formation of atoms and molecules after the big-bang to the present biosphere, eventually marginalised by the final death by freezing.

Since chemical kinetics advocates a syncretical grafting of time in a thermodynamic framework at the level of biophysical and biochemical processes that involve a restricted temperature range. As the margins of this range are approaching, the thermodynamical-like formulations inevitably need modification.

The theoretical framework elaborated in this and previous papers (Carvalho-Silva et al. 2019, 2020) becomes relevant because the scaling of the reaction rate constant as a function of the control variable  $\beta$  allows a simple renormalization scheme regarding the canonical definition of the activation energy  $E_a$ , the quantity which controls the coupling in a reactive process. Singularities at low temperatures are uniformly removed by the reciprocal of the activation energy  $E_a$ , the transitivity  $\gamma$ , and an effective coupling parameter  $d$  serves to cover the initially linear deviations from Arrhenius law that develop in the moderately low-temperature range.

Figure 1 points out at the insurgence of “unrenormalizable” ranges of temperature on the cold and hot sides: these general phenomena occur due to a variety of specific origins, hard to be treated by chemical kinetics. In a very different context, elementary particle investigations on a much higher-energy scale employ the so-called “ultraviolet cut off”: such marginalisation is actively investigated in high-energy physics (Weinberg 1995). In the view of Fig. 1, the “hot” marginalisation makes explicit the tendency to *anti*-behaviour: there is an increase of density of states emphasises the specificity of openings of additional channels. They may correspond to (molecular electronic,

roto-vibrational and translational) degrees of freedom, as well as to more drastic events, such as molecular fragmentations and ionizations (Leenson and Sergeev 1984). Aspects of this behaviour have been recently elucidated for tetratomic reactions (Coutinho et al. 2015, 2016, 2018) and for the conductivity of nanowires in proteins (Dahl et al. 2022; Guberman-Pfeffer 2022).

The present work has been focussed on the “cold” marginalisation, where the description of the reaction progress bifurcates into *sub*- and *super*-behaviour upon cooling (Fig. 1): only aspects are considered of the quantum mechanical phenomena regarding the approach to the Wigner’s limit as the temperature decreases. A variety of processes exhibiting *sub* and *super*-Arrhenius behaviour have been found and implementation of the present renormalization approach appears of interest.

The heuristic nature of the set of two coupled equations presented in this study enables access to classes of universality occurring for the tendency of tunnel dominated chemical reactions much before the Wigner’s limit. The fundamental significance of the microscopic origin of the curvatures depicted in Fig. 1 will be further evaluated in the future research through the incorporation of the definition of activation heat capacity (La Mer 1933; Hobbs et al. 2013), providing progress from a complementary predictive approach formulated in an extended thermodynamic language.

## Appendix

### Corrections and an equation for the thermodynamic limit

Most symbols used in this paper were introduced previously, specifically in (Carvalho-Silva et al. 2020), where in front of the last term of Eq. (9) and of the first member of Eq. (12) the prefactor  $A$  is missing.

The expansion of the Aquilanti–Mundim rate formula in the same Eq. (12) of (Carvalho-Silva et al. 2020) was given in power of  $\beta$  and it is valid to all given terms. Here, in order to exhibit the role of the deformation parameter  $d$  in the asymptotics of the thermodynamic limit ( $d \rightarrow 0$ ), for additional insights, the terms can be rearranged explicitly as a series in powers of  $d$  to the order  $\mathcal{O}(d^4)$ :

$$\begin{aligned}
 k_{AM}(\beta) &\equiv A(1-d\varepsilon^\ddagger\beta)^{\frac{1}{d}} \\
 &= Ae^{-\varepsilon^\ddagger\beta} \left[ 1 - \frac{1}{2}(\varepsilon^\ddagger\beta)^2 d - \left( \frac{1}{3}(\varepsilon^\ddagger\beta)^3 - \frac{1}{8}(\varepsilon^\ddagger\beta)^4 \right) d^2 \right. \\
 &\quad \left. - \left( \frac{1}{4}(\varepsilon^\ddagger\beta)^4 - \frac{1}{6}(\varepsilon^\ddagger\beta)^5 + \frac{1}{48}(\varepsilon^\ddagger\beta)^6 \right) d^3 + \mathcal{O}(d^4) \right]
 \end{aligned}
 \tag{A1}$$

**Acknowledgements** The authors acknowledge the Brazilian funding agencies Coordenação de Aperfeiçoamento de Pessoal de Nível Superior (CAPES) and Conselho Nacional de Desenvolvimento Científico e Tecnológico (CNPq) for financial support and CNPq Research Productivity Grant.

**Funding** Open access funding provided by Università degli Studi di Perugia within the CRUI-CARE Agreement. This research was funded by Goiás State agency FAPEG for the research funding programs (AUXÍLIO À PESQUISA COLABORATIVA FAPEG-FAPESP/GSP2019011000037).

**Data availability** None data available.

## Declarations

**Conflict of interest** The authors declare no conflict of interest.

**Open Access** This article is licensed under a Creative Commons Attribution 4.0 International License, which permits use, sharing, adaptation, distribution and reproduction in any medium or format, as long as you give appropriate credit to the original author(s) and the source, provide a link to the Creative Commons licence, and indicate if changes were made. The images or other third party material in this article are included in the article's Creative Commons licence, unless indicated otherwise in a credit line to the material. If material is not included in the article's Creative Commons licence and your intended use is not permitted by statutory regulation or exceeds the permitted use, you will need to obtain permission directly from the copyright holder. To view a copy of this licence, visit <http://creativecommons.org/licenses/by/4.0/>.

## References


- Abramowitz M, Stegun IA (1965) Handbook of mathematical functions: with formulas, graphs, and mathematical tables. Dover Publications
- Adam M, Calemma V, Galimberti F et al (2012) Continuum lumping kinetics of complex reactive systems. *Chem Eng Sci* 76:154–164. <https://doi.org/10.1016/j.ces.2012.03.037>
- Aquilanti V, Candori R, Cappelletti D et al (1990) Scattering of magnetically analyzed F (2P) atoms and their interactions with He, Ne, H<sub>2</sub> and CH<sub>4</sub>. *Chem Phys* 145:293–305. [https://doi.org/10.1016/0301-0104\(90\)89121-6](https://doi.org/10.1016/0301-0104(90)89121-6)
- Aquilanti V, Cavalli S, De Fazio D (1998) Hyperquantization algorithm. I. Theory for triatomic systems. *J Chem Phys* 109:3792–3804. <https://doi.org/10.1063/1.476979>
- Aquilanti V, Cavalli S, De Fazio D, Volpi A (2001) Theory of electronically nonadiabatic reactions: Rotational, Coriolis, spin-orbit couplings and the hyperquantization algorithm. *Int J Quantum Chem* 85:368–381. <https://doi.org/10.1002/qua.1527>
- Aquilanti V, Cavalli S, Pirani F et al (2001) Potential energy surfaces for F–H<sub>2</sub> and Cl–H<sub>2</sub>: long-range interactions and nonadiabatic couplings. *J Phys Chem A* 105:2401–2409. <https://doi.org/10.1021/jp003782r>
- Aquilanti V, Cavalli S, Simoni A et al (2004) Lifetime of reactive scattering resonances: Q-matrix analysis and angular momentum dependence for the F+H<sub>2</sub> reaction by the hyperquantization algorithm. *J Chem Phys* 121:11675–11690. <https://doi.org/10.1063/1.1814096>
- Aquilanti V, Cavalli S, De Fazio D et al (2005) Direct evaluation of the lifetime matrix by the hyperquantization algorithm: narrow resonances in the F+H<sub>2</sub> reaction dynamics and their splitting for nonzero angular momentum. *J Chem Phys* 123:054314. <https://doi.org/10.1063/1.1988311>
- Aquilanti V, Cavalli S, De Fazio D et al (2005) Benchmark rate constants by the hyperquantization algorithm. The F + H<sub>2</sub> reaction for various potential energy surfaces: features of the entrance channel and of the transition state, and low temperature reactivity. *Chem Phys* 308:237–253
- Aquilanti V, Mundim KC, Elango M et al (2010) Temperature dependence of chemical and biophysical rate processes: phenomenological approach to deviations from Arrhenius law. *Chem Phys Lett* 498:209–213. <https://doi.org/10.1016/j.cplett.2010.08.035>
- Aquilanti V, Mundim KC, Cavalli S et al (2012) Exact activation energies and phenomenological description of quantum tunneling for model potential energy surfaces. the F + H<sub>2</sub> reaction at low temperature. *Chem Phys* 398:186–191. <https://doi.org/10.1016/j.chemphys.2011.05.016>
- Aquilanti V, Coutinho ND, Carvalho-Silva VH (2017) Kinetics of low-temperature transitions and reaction rate theory from non-equilibrium distributions. *Philos Trans R Soc Lond A* 375:20160204. <https://doi.org/10.1098/rsta.2016.0201>
- Aquilanti V, Borges EP, Coutinho ND et al (2018) From statistical thermodynamics to molecular kinetics: the change, the chance and the choice. *Rend Lincei Sci Fis Nat* 28:787–802. <https://doi.org/10.1007/s12210-018-0749-9>
- Arroyo JI, Díez B, Kempes CP et al (2022) A general theory for temperature dependence in biology. *Proc Natl Acad Sci*. <https://doi.org/10.1073/pnas.2119872119>
- Astarita G (1989) Lumping nonlinear kinetics: apparent overall order of reaction. *AIChE J* 35:529–532. <https://doi.org/10.1002/aic.690350402>
- Astarita G, Ocone R (1988) Lumping nonlinear kinetics. *AIChE J* 34:1299–1309. <https://doi.org/10.1002/aic.690340808>
- Astarita G, Ocone R (1990) Continuous lumping in a maximum-mixedness reactor. *Chem Eng Sci* 45:3399–3405. [https://doi.org/10.1016/0009-2509\(90\)87145-1](https://doi.org/10.1016/0009-2509(90)87145-1)
- Bedjanian Y (2021) Rate constants for the reactions of F atoms with H<sub>2</sub> and D<sub>2</sub> over the temperature range 220–960 K. *Int J Chem Kinet* 53:527–535. <https://doi.org/10.1002/kin.21462>
- Callan CG (1970) Broken scale invariance in scalar field theory. *Phys Rev D* 2:1541. <https://doi.org/10.1103/PhysRevD.2.1541>
- Carrà S (2021) At the onset of bio-complexity: microscopic devils, molecular bio-motors, and computing cells. *Rend Lincei Sci Fis Nat* 32:215–232. <https://doi.org/10.1007/s12210-020-00971-1>
- Carvalho-Silva VH, Aquilanti V, de Oliveira HCB, Mundim KC (2017) Deformed transition-state theory: deviation from Arrhenius behavior and application to bimolecular hydrogen transfer reaction rates in the tunneling regime. *J Comput Chem* 38:178–188. <https://doi.org/10.1002/jcc.24529>
- Carvalho-Silva VH, Coutinho ND, Aquilanti V (2019) Temperature dependence of rate processes beyond Arrhenius and eyring: activation and transitivity. *Front Chem* 7:380. <https://doi.org/10.3389/fchem.2019.00380>
- Carvalho-Silva VH, Coutinho ND, Aquilanti V (2020) From the kinetic theory of gases to the kinetics of rate processes: on the verge of the thermodynamic and kinetic limits. *Molecules* 25:2098
- Cavalli S, Aquilanti V, Mundim KC, de Fazio D (2014) Theoretical reaction kinetics astride the transition between moderate and deep tunneling regimes: the F + HD case. *J Phys Chem A* 118:6632–6641. <https://doi.org/10.1021/jp503463w>
- Consolini G, Bruni F, Careri G (1992) Dissipative quantum tunneling of orientational defects in polycrystalline Ice. *Europhys Lett (EPL)* 19:547–551. <https://doi.org/10.1209/0295-5075/19/6/018>
- Coutinho ND, Silva VHC, De Oliveira HCB et al (2015) Stereodynamical origin of anti-arrhenius kinetics: negative activation energy

- and roaming for a four-atom reaction. *J Phys Chem Lett.* <https://doi.org/10.1021/acs.jpcclett.5b00384>
- Coutinho ND, Aquilanti V, Silva VHC et al (2016) Stereodirectional origin of anti-Arrhenius kinetics for a tetraatomic hydrogen exchange reaction: born-oppenheimer molecular dynamics for OH + HBr. *J Phys Chem A* 120:5408–5417
- Coutinho ND, Sanches-Neto FO, Carvalho-Silva VH et al (2018) Kinetics of the OH+ HCl→ H<sub>2</sub>O+ Cl reaction: rate determining roles of stereodynamics and roaming and of quantum tunneling. *J Comput Chem* 39:2508–2516
- Coutinho ND, Machado HG, Carvalho-Silva VH, da Silva WA (2021) Topography of the free energy landscape of Claisen-Schmidt condensation: solvent and temperature effects on the rate-controlling step—Pesquisa Google. *Phys Chem Chem Phys* 23:6738–6745
- Dahl PJ, Yi SM, Gu Y et al (2022) A 300-fold conductivity increase in microbial cytochrome nanowires due to temperature-induced restructuring of hydrogen bonding networks. *Sci Adv* 8:7193. [https://doi.org/10.1126/SCIADV.ABM7193/SUPPL\\_FILE/SCI-ADV.ABM7193\\_SM.PDF](https://doi.org/10.1126/SCIADV.ABM7193/SUPPL_FILE/SCI-ADV.ABM7193_SM.PDF)
- De Fazio D, Aquilanti V, Cavalli S et al (2006) Exact quantum calculations of the kinetic isotope effect: cross sections and rate constants for the F + HD reaction and role of tunneling. *J Chem Phys* 125:133109
- De Fazio D, Aquilanti V, Cavalli S et al (2008) Exact state-to-state quantum dynamics of the F+HD→HF (v' =2) +D reaction on model potential energy surfaces. *J Chem Phys.* <https://doi.org/10.1063/1.2964103>
- De Fazio D, Lucas JM, Aquilanti V, Cavalli S (2011) Exploring the accuracy level of new potential energy surfaces for the F + HD reactions: from exact quantum rate constants to the state-to-state reaction dynamics. *Phys Chem Chem Phys* 13:8571–8582. <https://doi.org/10.1039/c0cp02738c>
- De Fazio D, Cavalli S, Aquilanti V (2016) Benchmark quantum mechanical calculations of vibrationally resolved cross sections and rate constants on ab initio potential energy surfaces for the F + HD Reaction: comparisons with experiments. *J Phys Chem A.* <https://doi.org/10.1021/acs.jpca.6b01471>
- De Fazio D, Aquilanti V, Cavalli S (2019) Quantum dynamics and kinetics of the F + H<sub>2</sub> and F + D<sub>2</sub> reactions at low and ultra-low temperatures. *Front Chem* 7:328. <https://doi.org/10.3389/fchem.2019.00328>
- De Fazio D, Aquilanti V, Cavalli S (2020) Benchmark quantum kinetics at low temperatures toward absolute zero and role of entrance channel wells on tunneling, virtual states, and resonances: the F + HD reaction. *J Phys Chem A.* <https://doi.org/10.1021/acs.jpca.9b08435>
- Di Castro C, Jona-Lasinio G (1969) On the microscopic foundation of scaling laws. *Phys Lett A* 29:322–323. [https://doi.org/10.1016/0375-9601\(69\)90148-0](https://doi.org/10.1016/0375-9601(69)90148-0)
- Fowler RH, Guggenheim EA (1939) *Statistical thermodynamics: a version of statistical mechanics for students of physics and chemistry.* Macmillan
- Fu B, Xu X, Zhang DH (2008) A hierarchical construction scheme for accurate potential energy surface generation: an application to the F+H<sub>2</sub> reaction. *J Chem Phys* 129:011103. <https://doi.org/10.1063/1.2955729>
- Garn PD (1975) An examination of the kinetic compensation effect. *J Therm Anal* 7:475–478. <https://doi.org/10.1007/BF01911956>
- Glasstone S, Laidler KJ, Eyring H (1941) *The theory of rate processes: the kinetics of chemical reactions, viscosity, diffusion and electrochemical phenomena.* McGraw-Hill
- Corban AN (2021) Transition states and entangled mass action law. *Results Phys* 22:103922. <https://doi.org/10.1016/J.RINP.2021.103922>
- Guberman-Pfeffer MJ (2022) Assessing thermal response of redox conduction for *anti*-Arrhenius kinetics in a microbial cytochrome nanowire. *J Phys Chem B* 126:10083–10097. <https://doi.org/10.1021/acs.jpcc.2c06822>
- Hobbs JK, Jiao W, Easter AD et al (2013) Change in heat capacity for enzyme catalysis determines temperature dependence of enzyme catalyzed rates. *ACS Chem Biol* 8:2388–2393. <https://doi.org/10.1021/cb4005029>
- Honig JM, Spalek J (2018) *A primer to the theory of critical phenomena.* Elsevier Science, Amsterdam
- Kadanoff LP (2013) Relating theories via renormalization. *Stud Hist Philos Sci Part b* 44:22–39. <https://doi.org/10.1016/J.SHPSB.2012.05.002>
- Kummer A, Ocone R (2005) Statistical thermodynamic theory of the cell cycle: the state variables of a collection of cells. *Chem Phys Lett* 402:57–60. <https://doi.org/10.1016/j.cplett.2004.11.120>
- La Mer VK (1933) Chemical kinetics. The temperature dependence of the energy of activation. The entropy and free energy of activation. *J Chem Phys* 1:289. <https://doi.org/10.1063/1.1749291>
- Laidler KJ (1985) Chemical kinetics and the origins of physical chemistry. *Arch Hist Exact Sci* 32:43–75. <https://doi.org/10.1007/BF00327865>
- Laidler KJ (1996) A glossary of terms used in chemical kinetics, including reaction dynamics. *Pure Appl Chem* 68:149–192
- Leenson IA, Sergeev GB (1984) Negative temperature coefficient in chemical reactions. *Russ Chem Rev* 53:417–434. <https://doi.org/10.1070/RC1984v053n05ABEH003060>
- Lewis GN, Randall M (1922) *Thermodynamics and the free energy of chemical substances.* McGraw-Hill, London
- Machado HG, Sanches-Neto FO, Coutinho ND et al (2019) “Transitivity”: a code for computing kinetic and related parameters in chemical transformations and transport phenomena. *Molecules.* <https://doi.org/10.3390/molecules24193478>
- Nishiyama M, Kleijn S, Aquilanti V, Kasai T (2009) Mass spectrometric study of the kinetics of O<sub>2</sub> consumption and CO<sub>2</sub> production by breathing leaves. *Chem Phys Lett.* <https://doi.org/10.1016/j.cplett.2009.01.077>
- Nishiyama M, Kleijn S, Aquilanti V, Kasai T (2009) Temperature dependence of respiration rates of leaves, 18O-experiments and super-Arrhenius kinetics. *Chem Phys Lett* 482:325–329. <https://doi.org/10.1016/j.cplett.2009.10.005>
- Parisi G (1998) *Statistical field theory.* Avalon Publishing
- Piskulich ZA, Mesele OO, Thompson WH (2019) Activation energies and beyond. *J Phys Chem A* 123:7185–7194. <https://doi.org/10.1021/acs.jpca.9b03967>
- Rufino M, Guedes S (2022) Arrhenius activation energy and transitivity in fission-track annealing equations. *Chem Geol* 595:120779. <https://doi.org/10.1016/j.chemgeo.2022.120779>
- Sanches-Neto FO, Coutinho ND, Carvalho-Silva VH (2017) A novel assessment of the role of the methyl radical and water formation channel in the CH<sub>3</sub>OH + H reaction. *Phys Chem Chem Phys.* <https://doi.org/10.1039/c7cp03806b>
- Sanches-Neto FO, Ramos B, Lastre-Acosta AM et al (2021) Aqueous picloram degradation by hydroxyl radicals: unveiling mechanism, kinetics, and ecotoxicity through experimental and theoretical approaches. *Chemosphere* 278:130401. <https://doi.org/10.1016/j.chemosphere.2021.130401>
- Santin LG, Toledo EM, Carvalho-Silva VH et al (2016) Methanol solvation effect on the proton rearrangement of curcumin’s enol forms: an Ab Initio molecular dynamics and electronic structure viewpoint. *J Phys Chem C* 120:19923–19931. <https://doi.org/10.1021/acs.jpcc.6b02393>
- Silva VHC, Aquilanti V, De Oliveira HCB, Mundim KC (2013) Uniform description of non-Arrhenius temperature dependence of reaction rates, and a heuristic criterion for quantum tunneling vs classical non-extensive distribution. *Chem Phys Lett* 590:201–207
- Skouteris D, De Fazio D, Cavalli S, Aquilanti V (2009) Quantum stereodynamics for the two product channels of the F + HD reaction

- from the complete scattering matrix in the stereodirected representation. *J Phys Chem A* 113:14807–14812. <https://doi.org/10.1021/jp904972n>
- Sokolovski D, Sen SK, Aquilanti V et al (2007) Interacting resonances in the F+H<sub>2</sub> reaction revisited: complex terms, Riemann surfaces, and angular distributions. *J Chem Phys* 126:084305. <https://doi.org/10.1063/1.2432120>
- Stark K, Werner H (1996) An accurate multireference configuration interaction calculation of the potential energy surface for the F+H<sub>2</sub> → HF+H reaction. *J Chem Phys* 104:6515–6530. <https://doi.org/10.1063/1.471372>
- Stiller W (1989) Arrhenius equation and non-equilibrium kinetics: 100 years Arrhenius equation. Leipzig, Berlin
- Symanzik K (1971) Small-distance-behaviour analysis and Wilson expansions. *Commun Math Phys* 23:49–86. <https://doi.org/10.1007/BF01877596>
- Takayanagi T, Masaki N, Nakamura K et al (1987) The rate constants for the H+H<sub>2</sub> reaction and its isotopic analogs at low temperatures: Wigner threshold law behavior. *J Chem Phys* 86:6133. <https://doi.org/10.1063/1.452453>
- Tizniti M, Le Picard SD, Lique F et al (2014) The rate of the F + H<sub>2</sub> reaction at very low temperatures. *Nat Chem* 6:141–145. <https://doi.org/10.1038/nchem.1835>
- Tolman RC (1920) Statistical mechanics applied to chemical kinetics. *J Am Chem Soc* 42:2506–2528. <https://doi.org/10.1021/ja01457a008>
- Tolman RC (1927) Statistical mechanics with applications to Physics and Chemistry. First Published 1927, reprint 2013 in India by Isha Books, p 323
- Tsallis C (2009) Introduction to nonextensive statistical mechanics: approaching a complex world. Springer, New York
- van't Hoff JH (1884) Études de dynamique chimique. Frederik Muller, Amsterdam
- Vyazovkin S (2016) A time to search: finding the meaning of variable activation energy. *Phys Chem Chem Phys* 18:18643–18656. <https://doi.org/10.1039/C6CP02491B>
- Weinberg S (1995) The quantum theory of fields. Cambridge University Press
- Wigner E (1932) On the quantum correction for thermodynamic equilibrium. *Phys Rev* 40:749–759
- Wilson KG (1971) Renormalization group and critical phenomena. I. Renormalization group and the kadanoff scaling picture. *Phys Rev B* 4:3174–3183. <https://doi.org/10.1103/PhysRevB.4.3174>
- Wilson KG (1971) Renormalization group and critical phenomena. II. Phase-space cell analysis of critical behavior. *Phys Rev B* 4:3184–3205. <https://doi.org/10.1103/PhysRevB.4.3184>
- Wilson KG (1990) Ab initio quantum chemistry: a source of ideas for lattice gauge theorists. *Nucl Phys B Proc Suppl* 17:82–92. [https://doi.org/10.1016/0920-5632\(90\)90223-H](https://doi.org/10.1016/0920-5632(90)90223-H)
- Zuniga-Hansen N, Silbert LE, Calbi MM (2018) Breakdown of kinetic compensation effect in physical desorption. *Phys Rev E* 98:032128. <https://doi.org/10.1103/PhysRevE.98.032128>

**Publisher's Note** Springer Nature remains neutral with regard to jurisdictional claims in published maps and institutional affiliations.

## Authors and Affiliations

Valter H. Carvalho-Silva<sup>1,2</sup>  · Flávio O. Sanches-Neto<sup>2,3,4</sup> · Guilherme M. Leão<sup>1</sup> · Simonetta Cavalli<sup>5</sup> · Dario De Fazio<sup>6</sup> · Maria C. Nucci<sup>7,8</sup> · Vincenzo Aquilanti<sup>5,6</sup>

✉ Vincenzo Aquilanti  
vincenzo.aquilanti@unipg.it

Valter H. Carvalho-Silva  
fatiolog@ueg.br

Flávio O. Sanches-Neto  
flavio.neto@ifg.edu.br

Guilherme M. Leão  
guilherme.leao@educ.go.gov.br

Simonetta Cavalli  
simonetta.cavalli@unipg.it

Dario De Fazio  
dario.defazio@cnr.it

Maria C. Nucci  
mariaclara.nucci@unibo.it

<sup>2</sup> Universidade de Brasília, Caixa Postal 4478,  
Brasília 70904-970, Brazil

<sup>3</sup> Instituto Federal de Educação, Ciência e Tecnologia de  
Goiás, Valparaíso de Goiás, GO 72876-601, Brazil

<sup>4</sup> Instituto de Química, Universidade de Brasília, Caixa Postal  
4478, Brasília 70904-970, Brazil

<sup>5</sup> Dipartimento di Chimica, Biologia e Biotecnologie,  
Università di Perugia, 06123 Perugia, Italy

<sup>6</sup> Istituto di Struttura della Materia, Consiglio Nazionale delle  
Ricerche, 00016 Rome, Italy

<sup>7</sup> Dipartimento di Matematica, Università of Bologna,  
40126 Bologna, Italy

<sup>8</sup> Istituto Nazionale di Fisica Nucleare-Sezione di Perugia,  
06123 Perugia, Italy

<sup>1</sup> Laboratory for Modeling of Physical and Chemical Transformations, Research and Graduate Center, Goiás State University, Anápolis 75132-903, Brazil